VIBRATION TRANSMISSIBILITY BASED IDENTIFICATION OF SOFT VISCOELASTIC SYSTEMS

Anirudha Arvind Kulkarni[1], Rupal Srivastava[2], Bishakh Bhattacharya[3]
Department of Mechanical Engineering, Indian Institute of Technology Kanpur
Email:[2]rupalsri@iitk.ac.in, [3]bishakh@iitk.ac.in

ABSTRACT: The paper is aimed at developing mechanical models of viscoelastic materials on the basis of vibration transmissibility studies. At present, viscoelastic materials are characterized experimentally using rheometers, which work very well in very low to low frequency range. At high frequency range, on the other hand, Dynamic Mechanical Thermal Analyzers (DMTA) are used. However, this study requires materials to be stiff and self-supporting. Soft gel like materials are difficult to analyze in the DMTA machines directly. Often, steel backing plates are used as a substrate, however, the presence of a secondary substrate makes the analysis more complicated. This paper deals with the technique of analyzing soft viscoelastic materials based on transmissibility, which allows transition 'gel' like materials which are neither very soft, nor very stiff. Since the actual structural applications of some of the materials is envisaged to be at higher frequency level, the method developed in this paper will have more applicability in this scenario.

Keywords: Viscoelastic materials, vibration transmissibility, Standard Linear Solid model, Standard Linear Fluid model, Rheological models.

1. INTRODUCTION

The concept of perfectly elastic solids and perfectly viscous fluid are idealizations. Any real solid deviates from Hooke's law and any real fluid deviates from Newton's law, if measurements are done precisely. The deviations can be such that the stress in solids may not be only proportional to strain, but may depend on strain rate and other higher order derivatives of strain. Similarly, the stress in liquids may depend on higher order derivatives of strain, apart from being dependent on strain rate. These deviations are known as 'Time anomalies'. Materials showing time anomalies are the one which exhibit both solid like and fluid like behavior. Hence, such materials are called as Viscoelastic materials [1-3].

Mechanical properties of hydrogels were studied and determined experimentally by Anseth *et al.* [4] in 1995. Theory of rubber elasticity and viscoelasticity was used to study the behavior of hydrogels. Dynamic Mechanical Analysis (DMA) was used to study the viscoelastic behavior. Tensile tests were used to study the rubbery elastic behavior.

Investigation of microstructure and scaling of mechanical properties of dense colloidal gels was done by Rueb and Zukoshi [5] in 1996. Constant stress rheometer was used to determine mechanical properties. Effect of volume fraction and strength of inter-particle attraction on linear viscoelastic properties were investigated.

Textural, viscoelastic and muco-adhesive properties of cellulose polymer gels were studied by Jones *et al.* [6] in 1997. Oscillatory measurements were performed on a rheometer using frequency sweep tests. Effect of polymer concentration over viscoelastic functions was analyzed.

Empirical characterization of mechanical properties of alginate gels was done by Marco Mancini *et al.* [7] in 1999. The specimens of different shapes and dimensions were subjected to uniaxial compression testing. The stress-strain relationship was studied by varying the effective concentration, using power law model for correlation.

Rheological characterization of topical carbomer gels, neutralized to different pH was done by Islam *et al.* [8] in 2004. Viscoelastic properties, temperature dependency, yield strength and thixotropy of gels was analyzed using oscillatory, steady and transient shear measurements.

Dynamic mechanical properties of Agarose gels were studied by Chen *et al.* [9] in 2004. Dynamic Mechanical Analysis was used in frequency sweep shear sandwich mode. Fractional derivative model was used to explain the viscoelastic behavior.

Polyacrylamide (PAA) gels were characterized as an elastic model for food gels by Zhang *et al.* [10] in 2005. The shear modulus was determined as a function of temperature for viscoelastic PAA gels. Rheometric measurements were made to determine Linear Viscoelastic Region (LVR) and viscoelastic properties.

Behavior of food gels was studied using stress-strain tests by Tabilo-Munizaga and Barbosa-Canovas [11] in 2004. Small strain tests and large strain tests were performed on food gels. Small strain oscillatory tests were performed using rheometers to measure viscoelastic properties.

Properties of medium viscous and packable composites used in posterior composite restoration were studied by Lee *et al.* [12] in 2007. A vertical oscillation rheometer was employed to perform vertical compression and extension tests, simulating the clinical situation of composite filling.

Viscoelastic and poro-elastic mechanical characterization of hydrated gels was done by Galli *et al.* [13] in 2008. Indentation tests, unconfined compression tests and DMA were employed to examine the properties.

In this paper, first we will provide a brief description of the rheological models used for the analysis. Subsequently we will describe a new transmissibility based system identification technique. This will be followed by experimental results and conclusions.

2. RHEOLOGICAL MODELS

Behavior of viscoelastic materials is studied by applying forces (or deformation) as an input, and observing deformation (or forces) as output. The viscoelastic behavior can be assumed to be linear, if the acting forces (or deformations) are small, ensuring linear region of viscoelasticity [3]. Time dependent mechanical properties are found out from tests like creep and stress relaxation. In the creep test, the test material is subjected to a unit step of stress $\sigma_0 H(t)$, and the resulting strain response is recorded. The ratio of strain to stress at constant stress amplitude is called 'Creep Compliance', denoted by J(t). Similarly, the material is subjected to a unit step of strain $\sigma_0 H(t)$), and the resulting induced stresses are observed. The ratio of stress to strain, at constant strain amplitude is called 'Relaxation Modulus', denoted by G(t). Assuming inactivity of the material prior to t=0, we observe that both functions vanish at times t < 0.

Limiting values:
The behavior of viscoelastic material as $t \rightarrow 0^+$ is referred to as instantaneous (glassy) behavior, and as $t \rightarrow \infty$ is referred to as

equilibrium behavior. Hence, we commonly denote instantaneous compliance $J(t \rightarrow 0^+)$ by J_g and equilibrium compliance $J(t \rightarrow \infty)$ by J_e. Similarly, we denote instantaneous modulus $G(t \rightarrow 0^+)$ by G_g and equilibrium modulus by $G(t \rightarrow \infty)$ by G_e.

Both the functions are always positive. The creep compliance always increases, and relaxation modulus always decreases, as time goes from 0 to ∞ [2].

Three Parameter Model
Three parameter models exhibit more realistic material responses. They can be constructed considering different arrangements of springs and dash-pots. Two possible models considered are Standard Linear Solid (SLS) model and Standard Linear Fluid (SLF) model.

2.1 Standard Linear Solid (SLS) Model

When a spring is added in series with a K-V model, or in parallel with Maxwell model, we obtain SLS model (figure 2.1).
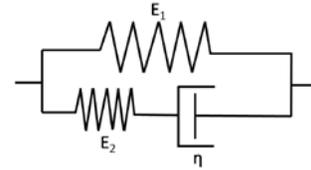

Figure 2.1: Standard Linear Solid model

These are called as solid models since they react instantaneously as elastic materials and recover completely upon unloading. The constitutive equation of SLS model is derived using integral formulations and Laplace transformations.

If stiffness of the spring in the Maxwell arm is E_2, stiffness of the spring in the arm parallel to Maxwell arm is E_1, and the damping co-efficient of the damper in the Maxwell arm is η, then the constitutive equation can be expressed as

$$\sigma + \frac{\eta}{E_2}\dot{\sigma} = E_1\epsilon + \eta \left(\frac{E_1+E_2}{E_2}\right)\dot{\epsilon} \qquad (1)$$

Creep Test
When a constant load σ_0 is applied, dash-pot takes time to respond. Both springs respond immediately [18], hence, the initial deformation becomes, $\dot{\epsilon} = \frac{\sigma_0}{E_1+E_2}$

The creep response of SLS model can be expressed as

$$\epsilon(t) = \left[\frac{1}{E_1} - \frac{E_2}{E_1(E_1+E_2)} e^{\frac{-t}{\tau_e}} \right] \sigma_0 \qquad (2)$$

where, $\tau_e = \frac{\eta(E_1+E_2)}{E_1 E_2}$ is the Retardation time.

Hence, the creep compliance is

$$J(t) = \frac{1}{E_1} - \frac{E_2}{E_1(E_1+E_2)} e^{\frac{-t}{\tau_e}} \qquad (3)$$

The instantaneous and equilibrium compliance of the SLS models are

$$J_g = \frac{1}{E_1+E_2}; \; J_e + \frac{1}{E_1} \qquad (4)$$

Consider a SLS model with parameters E_1=300Pa, E_2=1000Pa, η=40 NS/m^2. The creep compliance of this model is shown in figure 2.2. Variables on both the axes are made non-dimensional by dividing them by their maximum values.
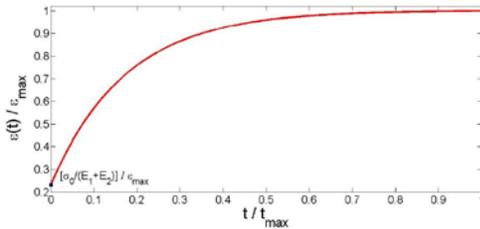

Figure 2.2: Creep response of SLS model

Thus, for a SLS model, we get $0 < J_g < J_e < \infty$

Stress Relaxation
When a constant strain E_0 is applied, the dash-pot does not offer any resistance to deformation. The stress is taken up by both the springs [1], hence, the initial condition becomes

$$\sigma_0 = (E_1 + E_2)\epsilon_0 \qquad (5)$$

The response of this SLS model to step strain is

$$\sigma(t) = \left(E_1 + E_2 e^{\frac{-t}{\tau_\sigma}} \right) \epsilon_0 \qquad (6)$$

Where $\tau_\sigma = \frac{\eta}{E_2}$ is the Relaxation time.

Hence the Relaxation modulus becomes

$$G(t) = E_1 + E_2 e^{\frac{-t}{\tau_\sigma}} \qquad (7)$$

The stress relaxation response of SLS model with above defined parameters will be as shown in figure 2.3.
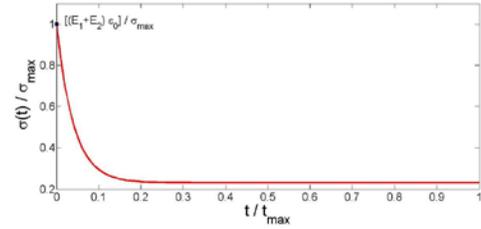

Figure 2.3: Stress relaxation of SLS model

The instantaneous and equilibrium modulus can be expressed as

$$G_g = (E_1 + E_2); \; G_e = E_1$$

We observe that $0 < G_e < G_g < \infty$

For a SLS model, the Retardation time is greater than the Relaxation time [2].

$$0 < \tau_\sigma < \tau_\epsilon < \infty$$

2.2 Standard Linear Fluid (SLF) Model

When a dash-pot is added in series with a K-V model, or in parallel with a Maxwell model, we get a SLF model (figure 2.4).
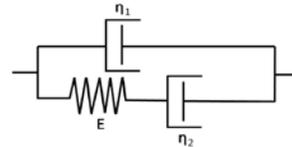

Figure 2.4: Standard Linear Fluid Model

These are called fluid models since it uses dash-pots and do not recover upon unloading.

If η_2 and η_1 represents the damping co-efficient of the damper in the Maxwell arm and arm parallel to Maxwell arm respectively, and E represents the spring stiffness of the spring in the Maxwell arm, then the constitutive equation of the SLF model can be expressed as

$$\sigma + \frac{\eta_2}{E}\dot{\sigma} = (\eta_1 + \eta_2)\dot{\epsilon} + \frac{\eta_1\eta_2}{E}\ddot{\epsilon} \qquad (8)$$

Creep Test

If a step load of σ_0 is applied to SLF model, the spring will try to stretch, but is held back by the dash-pots, which cannot react immediately. Since the spring does not change its length, all the initial stress is taken up by the dash-pot in the arm parallel to Maxwell arm. Hence the creep response curve starts with initial slope of $\frac{\sigma_0}{\eta_1}$ [1].

The creep response is given by

$$\epsilon(t) = \left(\frac{t}{\eta_1 + \eta_2} + \frac{\eta_2{}^2}{E(\eta_1 + \eta_2)^2}(1 - e^{\frac{-t}{\tau_\epsilon}})\right)\sigma_0 \qquad (9)$$

where, $\tau_\epsilon = \frac{\eta_1 \eta_2}{E(\eta_1 \eta_2)}$ is the Retardation time.

Hence the creep compliance is

$$J(t) = \frac{t}{\eta_1 + \eta_2} + \frac{\eta_2{}^2}{E(\eta_1 + \eta_2)^2}(1 - e^{\frac{-t}{\tau_\epsilon}}) \qquad (10)$$

Consider a SLF model with parameters E=300 Pa, η_1=15Ns/m^2, η_2=60Ns/m^2. The creep response of this model is displayed in figure 2.5. Variables on both the axes are made non-dimensional by dividing them by their maximum values.
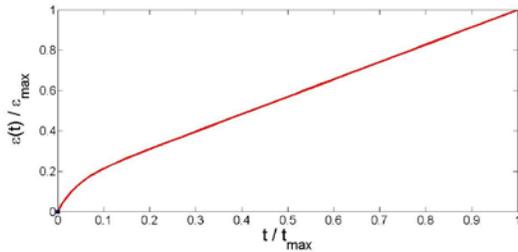

Figure 2.5: A typical creep response of SLF model

The instantaneous compliance is zero and SLF model does not have equilibrium compliance

$$J_g = 0 \; ; \; J_e = \infty$$

Stress Relaxation

When a constant strain E_0 is applied, the dash-pots do not offer any resistance to deformation. All the initial stress is taken up by the spring. Hence, the stress relaxation curve starts with an initial stress of $E\varepsilon_0$ which dies down exponentially. We get complete stress relaxation in case of SLF model [1]. The expression for stress relaxation is given by

$$\sigma(t) = E e^{\frac{-t}{\tau_\sigma}}\epsilon_0 \qquad (11)$$

Hence the relaxation modulus can be expressed as

$$G(t) = E e^{\frac{-t}{\tau_\sigma}} \qquad (12)$$

The time taken for complete relaxation is decided by Relaxation time τ_σ, which is equal to η_2/E. The stress relaxation response is shown in figure 2.6.
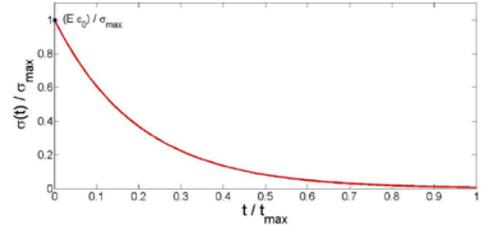

Figure 2.6: Stress relaxation of SLF model

The instantaneous and equilibrium modulus of SLF model are

$$G_g > 0 \; and \; G_e = 0$$

We observe that, for a SLF model $G_g > G_e$ Relaxation time must be greater than the retardation time [2].

$$0 < \tau_\epsilon < \tau_\sigma < \infty$$

3. NEW METHOD OF VISCOELASTIC SYSTEM IDENTIFICATION

The proposed method of system identification requires transmissibility data. The algorithm starts by approximating the test material into a 2 parameter Kelvin-Voight model, which is further refined into more realistic 3 parameter standard linear solid or standard linear fluid model. Three constraints are used to validate the model refinement results.

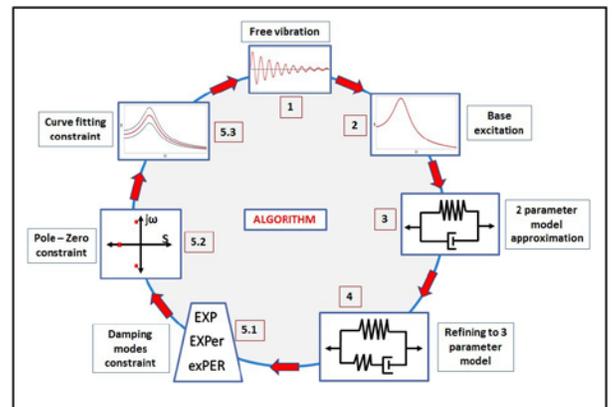The algorithm of the process is described in figure 3.1.

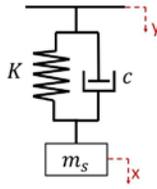Figure 3.1: System Identification algorithm

4

Figure 3.2: Base excitation of a K-V model

An expression for transmissibility of a K-V model is (figure 3.2) under base excitation is:

$$T = \sqrt{\frac{1+4\zeta^2\frac{\omega^2}{\omega_n^2}}{\left(1-\frac{\omega^2}{\omega_n^2}\right)^2+4\zeta^2\frac{\omega^2}{\omega_n^2}}} \tag{13}$$

where, ζ is the damping ratio and is the natural frequency of the model.

By substituting $\omega=\omega_d$ in the above equation, and using the relation $\omega_d = \omega_n\sqrt{(1-\zeta^2)}$, we get

$$T^2{}_{max} = \frac{1+4\zeta^2(1-\zeta^2)}{[1-(1-\zeta^2)]^2+[4\zeta^2(1-\zeta^2)]} \tag{14}$$

The next step in this method is to refine this 2 parameter model into a 3 parameter model adding one more parameter, spring constant K_c. The following figure 3.3 shows a typical Standard Linear Solid model which is a 3 parameter model.
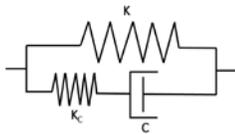

Figure 3.3: SLS model

Expression for transmissibility (T) of a Standard Linear Solid model (SLS) is

$$T = \sqrt{\frac{1+4\zeta^2\Omega^2(\lambda+1)^2}{(1-\Omega^2)^2+4\zeta^2\Omega^2[1+\lambda(1-\Omega^2)]^2}} \tag{15}$$

where, λ is the stiffness ratio (K/K_c). Values of ζ and ω_n are known from the 2 parameter model. From the transmissibility data we get values of T at different values of frequency ω. Thus in the transmissibility expression, the only unknown is stiffness ratio λ. Expression (15) is converted in terms of λ, which becomes a quadratic stiffness ratio equation.

For simplification, let
$$a = 4\zeta^2\Omega^2 \text{ and } b = 1 - \Omega^2$$

Thus, the quadratic equation of λ is obtained as

$$(ab^2T^2 - a)\lambda^2 + (2abT^2 - 2a)\lambda + (aT^2 + T^2b^2 - a - 1) = 0 \tag{16}$$

For each value of T obtained at a particular ω, a pair of roots of stiffness ratio λ are obtained. Value of stiffness of arm parallel to Maxwell arm (K) is already known from 2 parameter model. For each value of λ, a pair of values of the third parameter (K_c) are calculated. If the roots of λ are complex, that pair of roots are neglected.

A similar algorithm is followed for a Standard Linear Fluid model (SLF). The only change is in the transmissibility expression. For SLF model, it can be expressed as

$$T = \sqrt{\frac{4\zeta^2\Omega^2+(\beta+1)^2}{\frac{\Omega^2}{4\zeta^2}(4\zeta^2+\beta)^2+(\beta+1-\Omega^2)^2}} \tag{17}$$

where $\beta=c_1/c_2$ is the damping coefficient ratio.

4. EXPERIMENTAL RESULTS

4.1 System identification of PDMS block

The System Identification Algorithm was first tested on blocks of Poly-dimethylsiloxane (PDMS). PDMS comes from a group of polymeric organosilicon compounds. It is inert, non-flammable, non-toxic and optically transparent. It is also low in cost, easy to fabricate. Owing to these properties, PDMS finds its application in wide range of fields including bio-medical micro and Nano systems, microfluidics, optical MEMS, sensor applications, etc.

It is rigid enough to withstand its own weight. It can be categorized into the transition materials, which are neither very stiff, nor very soft. This is the reason why PDMS is selected as a test material for system identification.

The setup was excited with a Pseudo-Random excitation signal. The bandwidth used was 0 to 2 KHz for which the laser of the Polytec Scanning Vibrometer was used to record the displacement data.

The transmissibility curve, one obtained experimentally and other simulated after model identification for a PDMS block are shown in figure 4.1 and 4.2 respectively. The system identification algorithm identified SLS model as an appropriate model for this case.
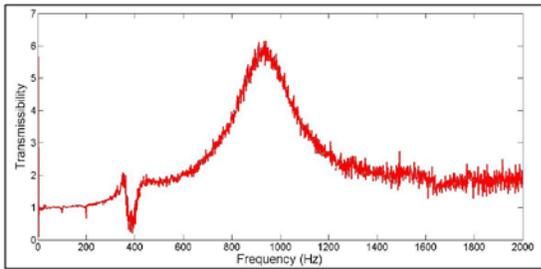
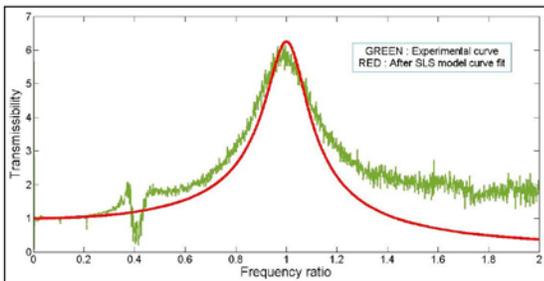Figure 4.1: Experimental Transmissibility plot

Figure 4.2: After SLS model curve fit

The values of modal parameters are listed in table 4.1.

Table 4.1 Result of PDMS block excitation

ω_d(Hz)	ζ	K(N/m)	c(Ns/m)	K_c(N/m)
940	0.0825	$2.305{\times}10^5$	6.4127	$4.436{\times}10^5$

4.2 System identification of Carbopol 940

A viscoelastic gel called Carbopol 940 was tested next in the base excitation experiments. But the experimental data did not suffice to characterize the samples. The response of top and bottom laser for Carbopol gel is displayed in figure 4.3. The top laser sensor records the displacement response of the test sample, while the bottom laser sensor records that of the container.
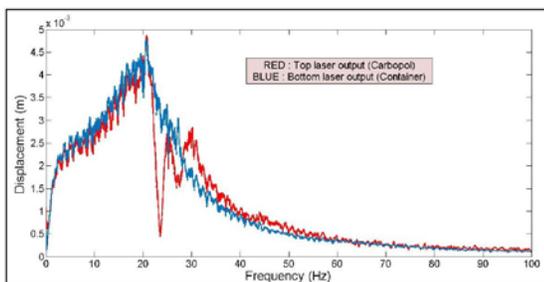

Figure 4.3: Displacement response of Carbopol gel and container

In the case of Carbopol gel, the gel surface follows the container movement up to the peak point. The waving motion of the gel surface in the axial direction can be seen in the figure.

The reason of occurrence of the initial peaks in top and bottom laser response is inertia of the container. The excitation signal sweeps across its designed bandwidth within few seconds. This rapid rate of base excitation is responsible for jerk, seen in the form of peak in the response. The response of the empty steel container subjected to the same excitation can be seen in figure 4.4.
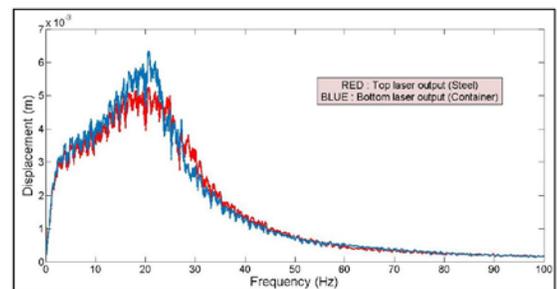

Figure 4.4: Displacement response of two points of an empty container

It can be seen that, both the top and bottom laser responses follow each other. Beyond the initial peak, there are no prominent peaks in either of the two response in frequency range of interest.

The transmissibility plot for Carbopol system are shown in figure 4.5. No prominent peaks are observed, and the data recorded are mixed with high noise.
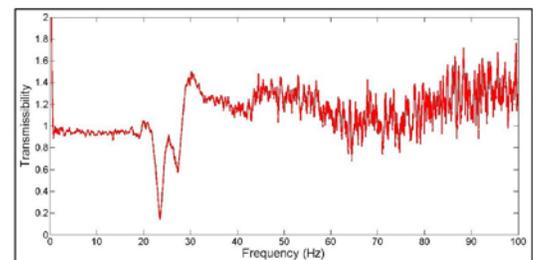

Figure 4.5: Transmissibility plot of Carbopol gel

5. CONCLUSION

The experimental studies however revealed the strength and weakness of the proposed technique. The new technique works quite well for gels with relatively high modulus of elasticity like PDMS. However, it is clear that the transmissibility based

method is not appropriate to characterize materials ranging from gel like substances to more fluid like substances.

The materials which are not rigid enough to support their own weight, have to be supported by the walls of the container. The inter-facial friction between walls of the container and the test sample make things even more complex.

For fluid like substances subjected to vertical excitement, sloshing phenomenon may be observed at the surface of the liquid. This is predicted from the sloshing response of the water filled tank subjected to vertical excitation studied by Amr M.I Sweedan [14], Housner [15].

The container's inertia is responsible for the initial peak observed in the individual laser responses. There is a certain bandwidth of frequency in which the inertial response is seen. Any test sample whose natural frequency would lie in that bandwidth would be difficult to characterize by this technique. Future works will extend the scope of experimental studies to include softer gels.

REFERENCES

1) Piaras Kelly. *Solid mechanics lecture notes*. The University of Auckland, 2013.
2) Francesco Mainardi and Giorgio Spada. Creep, relaxation and viscosity properties for basic fractional models in rheology. *The European Physical Journal Special Topics*, 193(1):133–160, 2011.
3) J.D. Ferry. *Viscoelastic properties of polymers*. Wiley, New York, 1st edition, 1961.
4) Kristi S Anseth, Christopher N Bowman, and Lisa Brannon-Peppas. Mechanical properties of hydrogels and their experimental determination. *Biomaterials*, 17(17):1647–1657, 1996.
5) CJ Rueb and CF Zukoski. Viscoelastic properties of colloidal gels. *Journal of Rheology (1978-present)*, 41(2):197–218, 1997.
6) David S Jones, A. David Woolfson, and Andrew F Brown. Textural, viscoelastic and mucoadhesive properties of pharmaceutical gels composed of cellulose polymers. *International journal of pharmaceutics*, 151(2):223–233, 1997.
7) Marco Mancini, Mauro Moresi, and Roberto Rancini. Mechanical properties of alginate gels: empirical characterization. *Journal of Food Engineering*, 39(4):369–378, 1999.
8) Mohammad T Islam, Nair Rodriguez-Hornedo, Susan Ciotti, and Chrisita Ackermann. Rheological characterization of topical carbomer gels neutralized to different ph. *Pharmaceutical research*, 21(7):1192– 1199, 2004.
9) Qingshan Chen, Bela Suki, and Kai-Nan An. Dynamic mechanical properties of agarose gels modeled by a fractional derivative model. *Journal of Bio-mechanical Engineering*, 126(5):666–671, 2004.
10) Junhua Zhang, Christopher R Daubert, and E Allen Foegeding. Characterization of polyacrylamide gels as an elastic model for food gels. *Rheologica acta*, 44(6):622–630, 2005.
11) Gipsy Tabilo-Munizaga and Gustavo V Barbosa-Cánovas. Rheology for the food industry. *Journal of Food Engineering*, 67(1):147–156, 2005.
12) In Bog Lee, Byeong Hoon Cho, Ho Hyun Son, and Chung Moon Um. Rheological characterization of composites using a vertical oscillation rheometer. *Dental materials*, 23(4):425–432, 2007.
13) Matteo Galli, Kerstyn SC Comley, Tamaryn AV Shean, and Michelle L Oyen. Viscoelastic and poroelastic mechanical characterization of hydrated gels. *Journal of Materials Research*, 24(03):973–979, 2009.
14) Amr MI Sweedan. Equivalent mechanical model for seismic forces in combined tanks subjected to vertical earthquake excitation. *Thin-Walled Structures*, 47(8):942–952, 2009.
15) George W Housner. The dynamic behavior of water tanks. *Bulletin of the seismological society of America*, 53(2):381–387, 1963.